Machine learning based on event-related oscillations of working memory differentiates between preclinical Alzheimer's disease and neurotypical aging

Ke Liao[1], Laura E. Martin[1,2], Sodiq Fakorede[3], William M. Brooks[1, 4, 5], Jeffrey M. Burns[4,5], Hannes Devos[3,5,6]

1. Hoglund Biomedical Imaging Center, University of Kansas Medical Center, Kansas City, KS, United States

2. Department of Population Health, University of Kansas Medical Center, Kansas City, KS, United States

3. Department of Physical Therapy, Rehabilitation Science, and Athletic Training, University of Kansas Medical Center, Kansas City, KS, United States

4. Department of Neurology, University of Kansas Medical Center, Kansas City, KS, United States

5. University of Kansas Alzheimer's Disease Research Center, University of Kansas Medical Center, Kansas City, KS, United States

6. Mobility Core, KU Center for Community Access, Rehabilitation Research, Education, and Service (KU-CARES), University of Kansas Medical Center, Kansas City, KS, United States

Abstract:

There is increasing evidence of the usefulness of electroencephalography (EEG) as an early neurophysiological marker of preclinical AD. Our objective was to apply machine learning approaches on event-related oscillations to discriminate preclinical AD from neurotypical controls. Twenty-two preclinical AD participants who were cognitively normal with elevated amyloid and 21 cognitively normal with no elevated amyloid controls completed n-back working memory tasks (n= 0, 1, 2). EEG signals were recorded through a high-density sensor net. The event-related spectral changes were extracted using the discrete wavelet transform in the delta, theta, alpha, and beta bands. The support vector machine (SVM) machine learning method was employed to classify participants, and classification performance was assessed using the Area Under the Curve (AUC) metric. The relative power of the beta and delta bands outperformed other frequency bands with higher AUC values. The 2-back task obtained higher AUC values

than the 0 and 1-back tasks. The highest AUC values were from the 2-back task beta band (AUC = 0.86) and delta bands (AUC = 0.85) nontarget data. This study demonstrates the promise of using machine learning on EEG event-related oscillations from working memory tasks to detect preclinical AD.

Keywords: Alzheimer's disease (AD), preclinical, spectral analysis, electroencephalography (EEG), discrete wavelet transform (DWT), machine learning, working memory, event-related oscillations (ERO), area under the receiver operating characteristic curve (AUC)

1. Introduction

Alzheimer's disease (AD) is one of the most common neurodegenerative diseases and the leading cause of dementia worldwide. About 50 million people were living with dementia and related disorders in 2018, and the prevalence is expected to increase to more than 150 million by the year 2050, according to the World Alzheimer Report (Patterson, 2018). This projected prevalence puts a tremendous burden on the health, long-term care, and hospice services for people with AD and dementia (Alzheimer's Association, 2023).

Electroencephalography (EEG) is an electrophysiological technique for recording brain electrical activity, which is a summation of the excitatory and inhibitory postsynaptic potentials of relatively large groups of neurons firing synchronously (Britton et al., 2016). EEG has been adopted for studying the neural dynamics across all stages of AD (Horvath et al., 2018; Maestú et al., 2019; Ouchani et al., 2021; Perez-Valero et al., 2021; Smailovic & Jelic, 2019). The high temporal sensitivity, non-invasiveness, cost-effectiveness, and accessibility make EEG suitable for

evaluating dynamic brain functioning and screening for early AD. These features of EEG may complement existing biomarkers such as tracing amyloid beta (Aβ) and tau in the blood, cerebrospinal fluid (CSF), or brain; assessing cortical hypometabolism on fluorodeoxyglucose positron emission tomography (FDG-PET); and evaluating brain atrophy on structural magnetic resonance imaging (MRI) (Jack et al., 2013; Jack et al., 2010).

Most EEG studies have focused on detecting changes in neural dynamics in people with diagnosed AD or mild cognitive impairment (MCI) (Ishii et al., 2017; Poza et al., 2014; Rossini et al., 2007). Individuals in these stages of AD already have marked cognitive impairments that may or may not affect daily life activities. However, few have investigated the preclinical phase of AD, which is characterized by early pathological changes related to AD in the presence of normal cognition (Gouw et al., 2017; Nakamura et al., 2018; Stomrud et al., 2010). Specifically, Stomrud et al. (2010) reported that total tau and phosphorylated tau (P-tau), and the combined P-tau/Aβ42 ratio measured in CSF correlated with relative EEG theta power, and slowing of cognitive speed correlated with increased relative theta power and high P-tau/Aβ42 ratio in cognitively normal older adults. Gouw et al. (2017) found that in participants with subjective cognitive decline, higher delta and theta power, and lower alpha power and peak frequency were associated with clinical progression over at least one year. Nakamura et al. (2018) demonstrated that in older adults with MCI and controls, increased Aβ levels were associated with higher alpha power in the medial frontal areas. In addition, increased delta power in the same region was associated with disease progression, entorhinal atrophy, and regional decrease in glucose metabolism.

The EEG power spectrum change is a promising neurophysiological biomarker to characterize the neural activity alterations associated with AD progression (Dauwels et al., 2011; Moretti, 2016; Stam et al., 2005). Spectral analysis can be applied to either resting-state EEG collected while participants are not doing any purposeful activity (Cassani et al., 2018; Moretti et al., 2004; Trinh et al., 2021) or during tasked-based EEG while participants perform a cognitive task (Chapman et al., 2011; Karrasch et al., 2006; Lai et al., 2010; Missonnier et al., 2007). The spectral changes under resting-state condition have been used successfully as features in studies on preclinical AD (Gouw et al., 2017; Nakamura et al., 2018; Stomrud et al., 2010). Spectral analysis for task-based studies have examined the event-related desynchronization/synchronization (ERD/ERS) (Babiloni et al., 2020; Fraga et al., 2018) and event-related oscillations (ERO) (Başar et al., 2013; Yener & Başar, 2013). Participants with MCI exhibited lower delta band oscillatory responses than neurotypical controls in oddball paradigms (Kurt et al., 2014; Yener et al., 2013). Participants with amnestic MCI demonstrated significantly lower theta power in a Sternberg recognition task than neurotypical controls (Cummins et al., 2008). Likewise, induced theta activity was significantly lower in progressive MCI than controls and stable MCI using n-back working memory tasks (Deiber et al., 2009). However, whether these task-related power spectrum rhythms also demonstrate in older adults with preclinical AD is unclear.

Machine learning offers a systematic approach to developing sophisticated, automatic, and objective classification frameworks for analyzing and recognizing complex and subtle patterns of high-dimensional data. Machine learning has been used in many MCI and AD studies (Mirzaei & Adeli, 2022; Pellegrini et al., 2018; Rathore et al., 2017; Tanveer et al., 2020) since it holds promise for improving the sensitivity and/or specificity of disease diagnosis (Rathore et al., 2017; Sajda, 2006). Among them, Petrosian et al. (2001) trained recurrent neural networks (RNN) on

resting-state EEG and obtained an accuracy under 90% in classifying participants with AD and controls. Fiscon et al. (2018) used decision trees classifiers on resting-state EEG and achieved 83%, 92%, and 79% accuracy in categorizing AD vs. controls, MCI vs. controls, and MCI vs. AD groups, respectively. You et al. (2020) proposed a cascade neural network on resting-state EEG with gait data and reached an accuracy rate of 91% in the three-way classification of controls, MCI, and AD. Khatun et al. (2019) used support vector machine (SVM) classifiers to predict MCI vs controls with 88% accuracy on auditory evoked potentials. However, no studies have used machine learning based on EEG oscillatory changes to classify participants with preclinical AD and controls.

In this study, we proposed to use event-related oscillations from working memory tasks, instead of resting-state EEG, to differentiate preclinical AD from neurotypical aging since previous studies have shown that memory activations can perform better than resting-state EEG in revealing spectral differences between participants with MCI and controls (van der Hiele et al., 2007). We hypothesized that machine learning approaches would detect early changes in spectral frequencies associated with AD and categorize participants with preclinical AD and controls with high accuracy.

2. Materials and Methods

2.1 Participants

The study cohort consisted of two groups of cognitively normal participants: 21 controls with no elevated Aβ and 22 preclinical AD adults with elevated Aβ. All participants were recruited exclusively from the University of Kansas Alzheimer's Disease Research Center during the period of May 30, 2018 to September 17, 2021. Participants were ineligible if they met any of

the following criteria based on their medical records: (1) currently using steroids, benzodiazepines, or neuroleptics; (2) had a history of substance abuse; (3) had a previous neurological disorder; or (4) had any contraindications to PET or EEG. The inclusion criteria consisted of the following: (1) being 65 years of age or older; (2) having a comprehensive understanding of all instructions given in English; (3) providing informed consent; and (4) having previously undergone an amyloid PET scan of the brain. The cerebral amyloid burden was determined using PET images acquired from a GE Discovery ST-16 PET/CT scanner subsequent to the administration of intravenous Florbetapir 18F-AV45 (370MBq), following a previously published protocol (Vidoni et al., 2021). Aβ status was determined by three experienced raters who independently interpreted all PET images without access to any clinical information, employing a method described in previous studies (Harn et al., 2017). The raters employed a combination of visual and quantitative data to establish whether a participant was classified as non-elevated or elevated (Clark et al., 2012; Joshi et al., 2012). The final status was determined based on the majority decision among the three raters. The median duration between the PET scan and EEG assessment was 1047 (823 - 1578) days. The participants' demographic information is shown in Table 1. The two groups did not differ with respect to age ($p = .60$), but there was a significant difference ($p < .01$) in the Montreal Cognitive Assessment (MoCA) scores (Nasreddine et al., 2005) with the MoCA scores for the control group (mean = 28.10) being higher than the preclinical AD group (mean = 26.05).

Table 1. Demographic information of study participants. Continuous variables were expressed as mean with standard deviation. The bold values were significant at $p < .01$ under the two-sample unequal variance t-test.

Group	Number	Sex (male: female)	Age	MoCA
Controls	21	8:13	74.38(5.93)	**28.10(1.89)**
Preclinical AD	22	6:16	73.52(4.52)	**26.05(2.79)**

2.2 Data acquisition and processing

The n-back working memory task (Fraga et al., 2018; Missonnier et al., 2006) was used to evoke event-related potentials. The participants were visually presented with a series of letters and instructed to respond in target condition trials when the current letter was ‘x’ in the 0-back task or was the same as the one presented in n (n = 1, 2) trials previously. In nontarget condition trials, participants were instructed to withhold responses (Devos et al., 2022; Devos et al., 2023).

The EEG signals were collected with a 256-channel high-density sensor net (Magstim EGI, Eugene, OR) at a sampling frequency of 1000 Hz and online referenced to the Cz channel. In offline processing, a digital filter of 0.5 to 30 Hz was applied, and the linked mastoid re-referencing was used. Non-neural activities were identified and removed using independent component analysis in EEGLAB (Delorme & Makeig, 2004). The clean data had 184 EEG channels with epoch length from -100ms to 1000ms in regard to stimulus onset. Only the trials with correct behavioral responses were included in the analysis. For more data cleaning and processing details, please see the original publications (Devos et al., 2022; Devos et al., 2023).

2.3 Spectral analysis

The individual averaged data were used for spectral analysis, and the wavelet-based relative power was obtained on each EEG channel. Wavelet transform is a time-frequency representation of the signal, which decomposes signals into different subbands (levels) with signal approximation and details. Compared to other spectral analyses like fast Fourier transform, wavelet transform can keep both the temporal and frequency information of the signal. As EEG is a non-stationary signal with changing properties over time, wavelet transform can catch the signal's transient features due to the scalability of its analyzing window (Strang & Nguyen, 1996). It enriches the analysis with more details than conventional time-frequency algorithms, such as short-time Fourier transform. Therefore, wavelet transform is a well-established signal representation and feature extraction technique for EEG processing (Faust et al., 2015; Frantzidis et al., 2014; Murugappan et al., 2010; Petrosian et al., 2001).

This study employed a multi-resolution decomposition method based on discrete wavelet transform (DWT) in power spectral analysis. In practice, DWT uses a low-pass filter $h(n)$ and a high-pass filter $g(n)$ to decompose the signal into its low-pass part (approximation) with its high-pass part (detail). In multi-level decomposition, DWT recursively decomposes approximation coefficients with the same pair of low and high-pass filters to the desired levels. The features extracted from the approximation and detailed coefficients at various levels can reveal the characteristics of the analyzed time series at different frequency bands. Figure 1 shows a schematic implementation of the DWT multi-resolution analysis using low-pass and high-pass filters.

Figure 1. Discrete wavelet transform implementation using low-pass and high-pass filters.

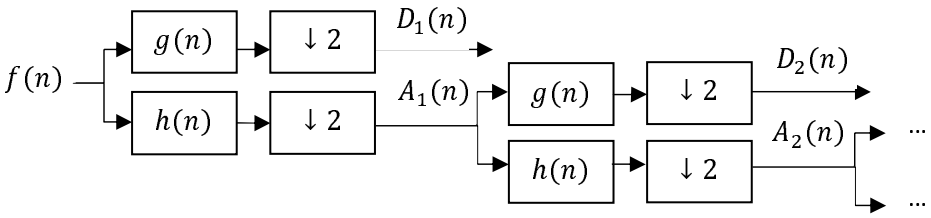

In Figure 1, only two levels of DWT decomposition were shown. The operation $\downarrow 2$ denoted a decimation of the signal by a factor of two.

Let $D_i(n)$ and $A_i(n)$ denote the detailed component and the approximate component on the decomposition level i, and the maximum level is M. The original EEG signal $f(n)$ could be represented as the sum of wavelet-based subbands in a multi-resolution analysis as

$$f(n) = D_1(n) + A_1(n) = D_1(n) + D_2(n) + A_2(n)$$
$$= \cdots = \sum_{i=1}^{M} D_i(n) + A_M(n) \quad (1)$$

Where $A_i(n) = A_{i+1}(n) + D_{i+1}(n)$ in two consecutive levels i and $i+1$.

A seven-level discrete wavelet transform decomposition ($M = 7$) was applied to the EEG signals. Only the DWT subbands obtained from the fifth to seventh levels were used in the analysis. Table 2 lists the decomposed signals A7, D7, D6, D5, which roughly corresponded to the EEG signal frequency bands of delta, theta, alpha, and beta, respectively. Accordingly, equation (1) could be calculated as follows:

$$f(n) = D_5(n) + D_6(n) + D_7(n) + A_7(n) \quad (2)$$

For each of the frequency bands mentioned above, the DWT relative spectral power $RP_i(i = 4, 5, 6, 7)$ was obtained as follows (Rosso et al., 2006; Wan et al., 2006; Wang et al., 2016):

$$RP_i = \frac{P_i}{P_t} \times 100\% = \frac{P_i}{\sum_{i=4}^{7} P_i} \times 100\% \quad (3)$$

Here the P_i was the absolute wavelet spectral power at level i that equaled to the sum of squared wavelet coefficients, and P_t was the total absolute spectral power. The DWT relative power RP is an index which characterizes the distribution of brain signal powers in the four frequency bands (i.e., delta, theta, alpha, and beta) in the n-back tasks.

Table 2. DWT subbands information and their corresponding EEG frequency bands.

DWT subbands	Frequency range corresponding EEG (Hz)	Corresponding frequency band (Hz)
D5	15.63-30	Beta (13-30)
D6	7.81-15.63	Alpha (8-13)
D7	3.91-7.81	Theta (4-8)
A7	0.5-3.91	Delta (0.5-4)

Among many wavelet families, the Daubechies wavelets have the properties of orthogonality and efficiency in filter implementation and were used in EEG spectral analysis(Subasi, 2007; Zarjam et al., 2015). Specifically, Daubechies wavelet with four vanishing moments (Db4) was adopted due to its suitability for analyzing EEG signals in AD in several studies (AlSharabi et al., 2022; Fiscon et al., 2018; Ghorbanian et al., 2013; Petrosian et al., 2001; Polikar et al., 2007). The Wavelet Toolbox of MATLAB (The MathWorks, Natick, Massachusetts) was employed in this study.

2.4 Classification approach

In order to decode group participants, we applied the multivariate pattern analysis (MVPA) (Grootswagers et al., 2017; King & Dehaene, 2014). The MVPA framework analyzes multivariates comprising multiple EEG channels or time points. MVPA usually encompasses a set of machine learning algorithms that provide an effective solution to reveal brain activation patterns associated with certain perceptual and cognitive states, specific stimuli, or other relevant information of participants.

We used the SVM machine learning method (Cortes & Vapnik, 1995) because it proved to perform well in previous AD studies compared to other classification algorithms (Chai et al., 2023; Khatri & Kwon, 2022; Menagadevi et al., 2023).

Due to the limited size of the dataset, we utilized a 5-fold cross-validation (CV) to validate the effectiveness of the classification (James, 2021). The complete datasets were randomly divided into two independent parts with an 80:20 ratio after data preparation, with 80% utilized for training and 20% used for testing. Then different data portions were used to test and train on subsequent iterations. This process was repeated until every fold of data served as the test set.

We assessed classifier performance using the receiver operating characteristic (ROC) curve analysis. The AUC (area under the ROC curve) value was used as it is more robust to imbalanced classes than the classification accuracy for binary classification (Treder, 2020). Generally, the classification performance was considered good with an AUC higher than 0.7 (Di

Flumeri et al., 2018; Fawcett, 2006). The AUC metric has been adopted in several AD diagnosis studies (Callahan et al., 2015; Liu et al., 2018; Moscoso et al., 2019).

We implemented this study by employing the MVPA-Light toolbox (Treder, 2020) for the multivariate analysis of EEG signals. The wavelet-based relative power extracted from different decomposition levels (i.e., delta, theta, alpha, and beta bands) on every EEG channel were used as features to represent EEG signals. The default implementation of SVM classifiers in MVPA-Light was used. The AUC values output from the toolbox were adopted as the performance metric. The cross-validation was repeated five times with new randomly assigned folds to achieve a more stable estimate of classification. The final performance was obtained by averaging all the repetitions.

2.5 Statistical analysis

In order to test the difference in the wavelet-based relative power between the two groups, a two-sample unequal variance t-test was used on each channel. Four midline EEG channels from the international 10-20 system, i.e., Fz, Cz, Pz, Oz, were selected to represent the relative power distribution among the central line. A threshold probability value of $p \leq .05$ was used to indicate statistical significance. Multiple comparisons were not corrected due to the exploratory nature of this study.

3. Results

The significant differences of target condition were most apparent in the 2-back task (Table 3). Relative delta band power at the channel locations Cz ($p = .05$) and Pz ($p = .02$) was lower in

the preclinical AD group compared to the control group. Conversely, relative theta (Pz, $p < .01$) and beta power (Fz, $p = .04$; Cz, $p = .02$; and Pz, $p = .02$) was higher in the preclinical group compared to the control group.

Fewer significant differences were observed in the 0-back and 1-back tasks. In the 0-back task, participants with preclinical AD showed greater power compared to controls in the theta band at channel Pz ($p = .04$) and in the beta band at channel Cz ($p = .01$).

Table 3. Wavelet-based relative power of target condition at midline EEG channels (mean and standard deviation, unit: percent). The bold values were significant at $p < .05$.

		0-back		1-back		2-back	
		Preclinical AD	Controls	Preclinical AD	Controls	Preclinical AD	Controls
delta	Fz	67.99(15.83)	72.43(16.85)	70.93(17.19)	75.27(15.13)	72.09(12.96)	79.31(12.70)
	Cz	67.24(15.59)	73.50(17.47)	71.35(15.60)	74.03(15.44)	**71.30(13.27)**	**79.93(14.47)**
	Pz	79.71(13.37)	82.78(9.38)	79.95(11.14)	84.06(11.92)	**73.61(17.25)**	**85.06(11.25)**
	Oz	79.87(11.79)	79.64(8.15)	77.15(13.89)	82.93(10.20)	76.83(13.42)	78.90(12.57)
theta	Fz	16.87(10.80)	14.78(11.79)	17.09(13.12)	14.82(10.59)	16.66(10.87)	11.76(7.56)
	Cz	17.32(9.79)	13.72(11.53)	17.56(14.42)	13.60(10.38)	16.73(11.24)	11.27(9.86)
	Pz	**9.69(5.25)**	**6.54(3.99)**	9.81(7.36)	6.16(6.61)	**11.48(8.45)**	**5.05(3.88)**
	Oz	8.83(5.92)	9.74(7.02)	10.09(7.69)	6.53(4.01)	9.51(7.02)	8.20(5.99)
alpha	Fz	11.08(7.46)	9.84(7.42)	8.68(8.45)	7.50(6.03)	7.09(4.23)	6.36(6.80)
	Cz	11.00(8.81)	10.21(7.40)	7.98(6.25)	9.66(6.96)	8.11(4.89)	6.43(5.59)
	Pz	8.18(9.07)	7.78(4.77)	6.82(3.63)	7.41(5.85)	9.68(8.63)	7.33(7.88)
	Oz	8.61(7.19)	7.60(3.93)	8.88(6.30)	7.43(5.88)	8.93(6.27)	9.25(9.24)
beta	Fz	4.07(3.57)	2.96(2.06)	3.30(1.76)	2.42(2.04)	**4.16(2.70)**	**2.57(2.05)**
	Cz	**4.45(2.71)**	**2.58(1.63)**	3.11(1.93)	2.71(2.46)	**3.86(2.21)**	**2.37(1.55)**

	Pz	2.42(1.67)	2.89(1.89)	3.42(2.48)	2.37(2.06)	**5.23(4.82)**	**2.55(1.60)**
	Oz	2.69(2.37)	3.02(1.16)	3.88(2.84)	3.12(2.45)	4.72(4.01)	3.65(2.26)

The relative power of the nontarget condition in Table 4 showed a similar pattern to the target condition in Table 3.

Relative power in the delta band was lower in the preclinical group compared to the control group, while the reverse was true in theta, alpha, and beta bands at the midline channels. In the 2-back task, the preclinical group exhibited lower delta band power at all channels: Fz ($p = .03$), Cz ($p < .01$), Pz ($p = .04$), and Oz ($p = .05$). The power was significantly higher in the preclinical group than the controls in the theta band at Cz ($p= .03$), in the alpha band at Cz ($p = .02$) and Oz ($p = .03$), and in the beta band at Fz ($p = .02$) and Cz ($p < .01$).

None of the channels showed a significant difference between the two groups in the 0-back and 1-back tasks.

Table 4. Wavelet-based relative power of nontarget condition at midline EEG channels (mean and standard deviation, unit: percent). The bold values were significant at $p < .05$.

		0-back		1-back		2-back	
		Preclinical AD	Controls	Preclinical AD	Controls	Preclinical AD	Controls
delta	Fz	64.71(15.18)	69.16(18.53)	69.89(18.22)	73.11(17.82)	**66.83(15.85)**	**77.65(15.06)**
	Cz	65.92(15.54)	71.79(18.58)	70.49(12.98)	74.93(15.52)	**64.30(14.60)**	**80.31(15.35)**
	Pz	71.90(15.80)	79.67(10.07)	79.60(10.88)	80.67(15.82)	**71.45(16.96)**	**82.30(14.98)**

	Oz	72.21(17.07)	75.34(15.03)	77.90(13.08)	80.50(10.99)	**71.07(17.22)**	**80.58(12.27)**
theta	Fz	23.02(12.32)	20.22(13.62)	20.90(14.14)	18.91(13.76)	22.12(12.96)	15.61(11.86)
	Cz	22.47(12.17)	17.66(13.29)	19.51(11.34)	16.79(12.82)	**22.39(13.18)**	**13.11(13.55)**
	Pz	13.77(9.73)	9.39(6.19)	10.89(8.17)	8.90(9.40)	12.77(10.37)	7.67(7.16)
	Oz	12.97(9.48)	12.32(7.29)	11.65(9.73)	8.81(3.76)	12.22(9.03)	9.73(8.40)
alpha	Fz	8.22(6.08)	8.01(7.30)	6.91(6.73)	6.22(6.59)	8.04(5.89)	5.08(4.68)
	Cz	8.12(6.31)	8.01(8.07)	7.39(6.33)	6.53(5.60)	**9.35(6.86)**	**5.16(3.54)**
	Pz	10.43(8.17)	7.71(4.74)	7.34(5.48)	7.99(9.17)	11.03(8.85)	7.22(7.15)
	Oz	11.00(7.64)	8.30(6.86)	8.15(4.55)	8.03(8.37)	**11.88(8.54)**	**6.78(6.14)**
beta	Fz	4.05(3.30)	2.60(1.39)	2.30(1.48)	1.77(1.34)	**3.02(2.07)**	**1.66(1.34)**
	Cz	3.49(2.27)	2.54(1.77)	2.61(2.09)	1.76(1.43)	**3.97(3.12)**	**1.41(0.76)**
	Pz	3.89(3.41)	3.23(2.70)	2.17(1.43)	2.43(2.38)	4.75(5.77)	2.81(3.03)
	Oz	3.82(3.50)	4.04(3.52)	2.30(1.72)	2.67(1.96)	4.82(4.79)	2.92(2.57)

The AUC topographies showed higher values in the 2-back compared to the 0-back and 1-back tasks (Figure 2). The 0-back and 1-back tasks had similar AUC performances, with no consistent AUC contours in these tasks.

Figure 2. Topographies of AUC values of target condition in the 0-back, 1-back, and 2-back tasks. Channels with AUC higher than 0.7 were contoured.

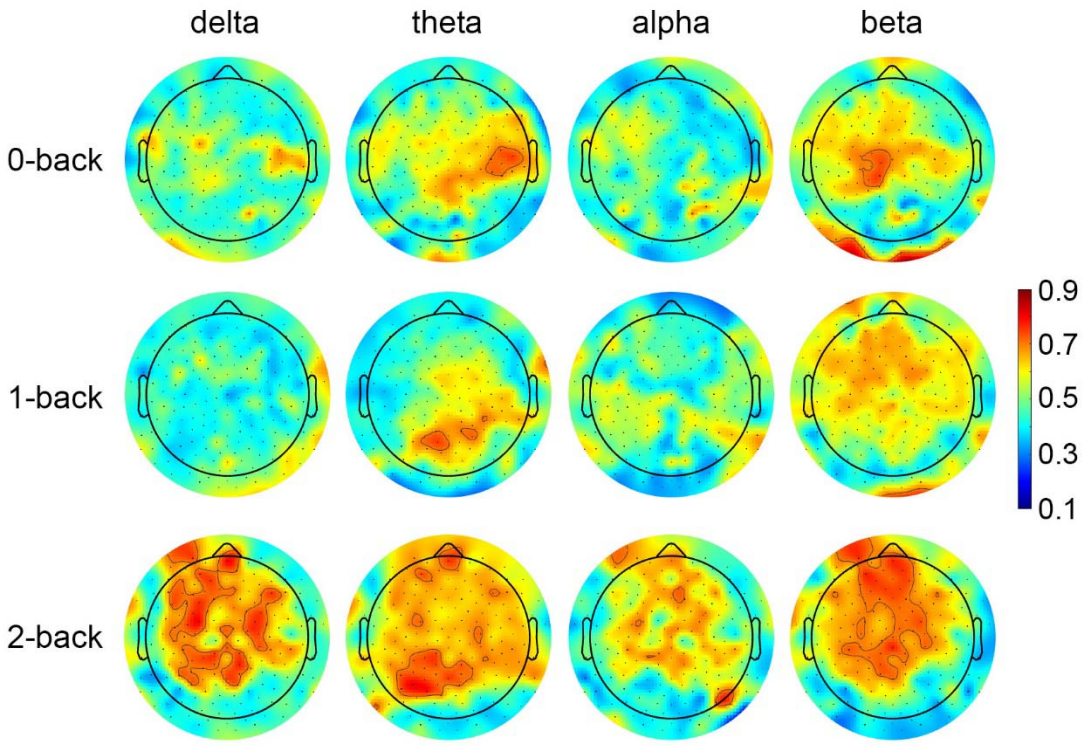

Figure 2 shows AUC value topographies of all frequency bands (i.e., delta, theta, alpha, and beta) of the n-back target condition.

In the 2-back task, high AUC values (>0.7) were observed in the frontal, central, and parietal areas. Specifically, Table 5 showed that the highest AUC values in the 2-back task were observed in the theta (AUC = 0.81) and delta bands (AUC = 0.80), followed by the beta band (AUC = 0.77). The alpha band was the lowest (highest AUC = 0.72).

The AUC topographies of the nontarget condition, shown in Figure 3, followed a consistent pattern as in Figure 2, with the 2-back task achieving higher AUC values than the 0-back and 1-back tasks. The delta and beta bands had the highest AUCs (0.85 in the delta band and 0.86 in the beta band, 2-back data, Table 5), followed by the theta band (AUC = 0.81). The alpha band

had the lowest value (highest AUC = 0.78). The contours of channels with AUC higher than 0.7 covered the frontal, central, and parietal brain areas (2-back task).

Figure 3. Topographies of AUC values of nontarget condition in the 0-back, 1-back, and 2-back tasks. Channels with AUC higher than 0.7 were contoured.

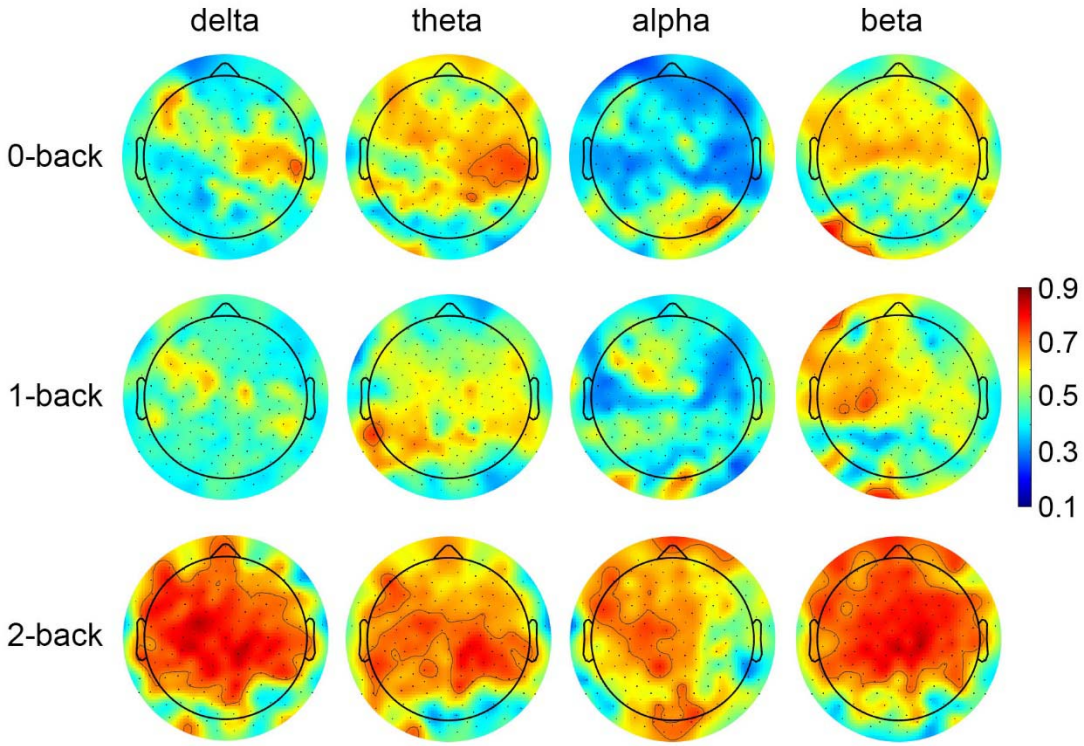

Table 5 shows the highest AUC values of all frequency bands in 0, 1 and 2-back tasks.

The AUC of the 2-back task grossly exhibited higher values than the 0-back and 1-back tasks in each frequency band for both target and nontarget conditions.

The nontarget condition generally obtained higher AUC values than the target condition. The highest AUC values were from 2-back nontarget beta band data (AUC = 0.86), followed by the delta band (AUC = 0.85).

Table 5. The highest AUC values of all frequency bands in n-back tasks for target and nontarget conditions (mean with standard deviation).

		delta	theta	alpha	beta
0-back	target	0.68(0.17)	0.75(0.19)	0.69(0.23)	0.75(0.14)
	nontarget	0.71(0.19)	0.74(0.16)	0.73(0.18)	0.78(0.17)
1-back	target	0.63(0.14)	0.75(0.16)	0.67(0.20)	0.68(0.19)
	nontarget	0.66(0.12)	0.76(0.16)	0.67(0.17)	0.75(0.16)
2-back	target	0.80(0.13)	0.81(0.15)	0.72(0.17)	0.77(0.17)
	nontarget	0.85(0.13)	0.81(0.15)	0.78(0.17)	0.86(0.12)

4. Discussion

The outcomes of this study underscore the utilization of machine learning approaches, employing EEG spectral features from task-based data, to distinguish cognitively normal older adults with preclinical AD from cognitively normal controls. While a few studies have noted task-related EEG modifications in older adults with an elevated risk of AD (Arakaki et al., 2019; Choi et al., 2023), these investigations have not incorporated machine learning techniques for group classification. Our study addresses this gap by providing validation that memory-related EEG oscillations can signify neurocognitive changes preceding clinical diagnosis. Furthermore, we establish that these EEG patterns encompass substantial information for the early identification of older adults at risk of AD.

The highest classification performance of this study was obtained in the beta band (AUC = 0.86) and the delta band (AUC = 0.85), which were almost identical (2-back task, nontarget data in Table 5). Both beta and delta oscillations are believed to be related to working memory function (Harmony, 2013; Harmony et al., 1996; Miller et al., 2018; Schmidt et al., 2019; Spitzer & Haegens, 2017). Our results revealed that the beta and delta EEG bands carried the most information on spectral changes between adults with preclinical AD and controls. This is in line with Fernández et al. (2006), who identified that relative power in the beta (16-28 Hz) and the delta (2-4 Hz) frequency bands were the most sensitive variables in differentiating AD patients and controls.

Our finding that the delta-band relative power of the 2-back task in the preclinical AD group was lower than the control group was in accordance with our previous study (Devos et al., 2022), as well as the relative power increase of other frequency bands in the preclinical AD group at Cz, Pz, and Oz channels (Tables 3 and 4). The overall spectral shift towards decreased power in the low-frequency delta band and increased power in the high-frequency beta bands in the preclinical AD group are consistent with neural hyperexcitability, a finding increasingly reported in the literature (Devos et al., 2022; Targa Dias Anastacio et al., 2022). Although the drivers of this increased neural excitability in this preclinical phase of AD are still unclear (Targa Dias Anastacio et al., 2022), studies in animal models of AD have found a strong link between hyperexcitability and Aβ accumulation near the hyperexcitable neurons (Busche & Konnerth, 2016). Previous EEG studies also reported that individuals with MCI have higher power from theta to beta bands than controls during working memory tasks (Jiang, 2005). This finding aligns with our results on theta, alpha, and beta bands power, in which the preclinical AD group shows larger values than the control group, and most of the significant differences may be elicited with more difficult working memory tasks such as the 2-back task (Tables 3 and 4).

The AUC topographies showed higher values in the front-centro-parietal brain areas (Figures 2 and 3, delta and beta bands, 2-back task). This region included the frontal lobe, where the event-related potential (P3 component) was found to provide good reliability for studying the effect of Aβ on neural transmission in preclinical AD in our previous study (Devos et al., 2020) since the frontal lobe is tightly associated with working memory (Kondo et al., 2004). One study that identified amnestic MCI using convolutional neural networks also showed that the channels in the frontal lobe were with a top representation of patients' cognitive states (Li et al., 2022). The possible mechanism of delivering high AUCs in the front-centro-parietal areas is that working memory relies on different functional sub-systems, and it is attributable to the coordination of disparate brain areas, in particular frontal and parietal regions (Imaruoka et al., 2005; Owen et al., 2005).

When comparing performance between tasks, the 2-back task achieved higher AUCs than the 0-back and 1-back tasks (Table 5). Previous studies suggested that different work or memory load levels could invoke spectral power alterations in various frequency bands (Baldwin & Penaranda, 2012; Brouwer et al., 2012; Christensen et al., 2012; Michels et al., 2010; Pesonen et al., 2007). We assume that the high workload task, i.e., 2-back, might have the potential to fully exploit the working memory capacity and produce more discriminatory EEG oscillatory activity patterns between the preclinical AD and control groups.

In the current study, the AUC of the classifier with the best performance was 0.86. Previous studies reported highest AUC values ranging between from 0.80 to 0.89 in classifying AD vs. controls (Babiloni et al., 2016; Chai et al., 2019; Chedid et al., 2022; de Haan et al., 2008; Ding et al., 2022; Fernández et al., 2006; Meghdadi et al., 2021; Trambaiolli et al., 2011), and

between 0.60 and 0.81 in classifying MCI vs. controls (Ding et al., 2022; Gómez et al., 2009; Meghdadi et al., 2021; Sibilano et al., 2023). Considering that those studies investigated disease stages of AD with apparent cognitive impairments, our model achieved similar classification performance in a preclinical phase of AD with normal cognition. Our results suggest that electrophysiological changes could occur prior to cognitive changes, and the event-related oscillations could serve as easy, relatively inexpensive, yet accurate markers of preclinical AD.

Although our study compares well with the participant size of previous studies (Chai et al., 2019; Gómez et al., 2009; Mazaheri et al., 2018; Trambaiolli et al., 2011), we acknowledge the limitation that the size of the participants is small, and a future study with larger-scale samples is needed. Furthermore, EEG power spectra could change during the course of disease. In a 2.5-year follow-up study of AD, an increase of delta and theta activities and a decrease of alpha and beta activities were reported (Coben et al., 1985). A longitudinal study is warranted to confirm the use of EEG as an accurate marker of cognitive decline. Finally, the time interval between PET and EEG scans was relatively long. We cannot rule out that some participants with preclinical AD might have converted to MCI. Nevertheless, the average MOCA scores were higher than 26, indicating no cognitive impairments in the preclinical AD group.

5. Conclusion

In this study, an SVM-based machine learning model was built to discriminate preclinical AD and neurotypical older adults, using EEG data from n-back working memory tasks. The event-related oscillation was analyzed in all frequency bands using features extracted from discrete wavelet transform. Our results showed that relative power from the beta and delta bands,

particularly in the 2-back task, can achieve higher classification performance than other frequency bands and less demanding tasks. This study demonstrates that machine learning based on memory-related power spectral features are capable of characterizing the brain activities change associated with preclinical AD from healthy controls. Our results imply that EEG oscillations may reveal pathophysiological changes in the earliest stage of AD when no cognitive impairments are apparent.

Reference

AlSharabi, K., Salamah, Y. B., Abdurraqeeb, A. M., Aljalal, M., & Alturki, F. A. (2022). EEG Signal Processing for Alzheimer's Disorders Using Discrete Wavelet Transform and Machine Learning Approaches. *IEEE Access*, *10*, 89781-89797. https://doi.org/10.1109/ACCESS.2022.3198988

Alzheimer's Association. (2023). 2023 Alzheimer's disease facts and figures. *Alzheimers Dement*, *19*(4), 1598-1695. https://doi.org/10.1002/alz.13016

Arakaki, X., Lee, R., King, K. S., Fonteh, A. N., & Harrington, M. G. (2019). Alpha desynchronization during simple working memory unmasks pathological aging in cognitively healthy individuals. *PLoS One*, *14*(1), e0208517. https://doi.org/10.1371/journal.pone.0208517

Babiloni, C., Blinowska, K., Bonanni, L., Cichocki, A., De Haan, W., Del Percio, C., Dubois, B., Escudero, J., Fernández, A., Frisoni, G., Guntekin, B., Hajos, M., Hampel, H., Ifeachor, E., Kilborn, K., Kumar, S., Johnsen, K., Johannsson, M., Jeong, J., . . . Randall, F. (2020). What electrophysiology tells us about Alzheimer's disease: a window into the synchronization and connectivity of brain neurons. *Neurobiol Aging*, *85*, 58-73. https://doi.org/10.1016/j.neurobiolaging.2019.09.008

Babiloni, C., Triggiani, A. I., Lizio, R., Cordone, S., Tattoli, G., Bevilacqua, V., Soricelli, A., Ferri, R., Nobili, F., Gesualdo, L., Millán-Calenti, J. C., Buján, A., Tortelli, R., Cardinali, V., Barulli, M. R., Giannini, A., Spagnolo, P., Armenise, S., Buenza, G., . . . Del Percio, C. (2016). Classification of Single Normal and Alzheimer's Disease Individuals from Cortical Sources of Resting State EEG Rhythms. *Front Neurosci*, *10*, 47. https://doi.org/10.3389/fnins.2016.00047

Baldwin, C. L., & Penaranda, B. N. (2012). Adaptive training using an artificial neural network and EEG metrics for within- and cross-task workload classification. *NeuroImage*, *59*(1), 48-56. https://doi.org/10.1016/j.neuroimage.2011.07.047

Başar, E., Başar-Eroğlu, C., Güntekin, B., & Yener, G. G. (2013). Brain's alpha, beta, gamma, delta, and theta oscillations in neuropsychiatric diseases: proposal for biomarker strategies. *Suppl Clin Neurophysiol*, *62*, 19-54. https://doi.org/10.1016/b978-0-7020-5307-8.00002-8

Britton, J. W., Frey, L. C., Hopp, J. L., Korb, P., Koubeissi, M. Z., Lievens, W. E., Pestana-Knight, E. M., & St. Louis, E. K. (2016). *Electroencephalography (EEG): An Introductory Text and Atlas of Normal and Abnormal Findings in Adults, Children, and Infants*. American Epilepsy Society.

Brouwer, A.-M., Hogervorst, M. A., van Erp, J. B. F., Heffelaar, T., Zimmerman, P. H., & Oostenveld, R. (2012). Estimating workload using EEG spectral power and ERPs in the n-back task. *Journal of Neural Engineering*, *9*(4), 045008. https://doi.org/10.1088/1741-2560/9/4/045008

Busche, M. A., & Konnerth, A. (2016). Impairments of neural circuit function in Alzheimer's disease. *Philos Trans R Soc Lond B Biol Sci*, *371*(1700). https://doi.org/10.1098/rstb.2015.0429

Callahan, B. L., Ramirez, J., Berezuk, C., Duchesne, S., Black, S. E., & for the Alzheimer's Disease Neuroimaging, I. (2015). Predicting Alzheimer's disease development: a comparison of cognitive criteria and associated neuroimaging biomarkers. *Alzheimer's Research & Therapy*, *7*(1), 68. https://doi.org/10.1186/s13195-015-0152-z

Cassani, R., Estarellas, M., San-Martin, R., Fraga, F. J., & Falk, T. H. (2018). Systematic Review on Resting-State EEG for Alzheimer's Disease Diagnosis and Progression Assessment. *Dis Markers*, *2018*, 5174815. https://doi.org/10.1155/2018/5174815

Chai, J., Wu, R., Li, A., Xue, C., Qiang, Y., Zhao, J., Zhao, Q., & Yang, Q. (2023). Classification of mild cognitive impairment based on handwriting dynamics and qEEG. *Computers in Biology and Medicine*, *152*, 106418. https://doi.org/10.1016/j.compbiomed.2022.106418

Chai, X., Weng, X., Zhang, Z., Lu, Y., Liu, G., & Niu, H. (2019). Quantitative EEG in Mild Cognitive Impairment and Alzheimer's Disease by AR-Spectral and Multi-scale Entropy Analysis. In L. Lhotska, L. Sukupova, I. Lacković, & G. S. Ibbott (Eds.), *World Congress on Medical Physics and Biomedical Engineering 2018*. Springer Singapore. https://doi.org/10.1007/978-981-10-9038-7_29

Chapman, R. M., McCrary, J. W., Gardner, M. N., Sandoval, T. C., Guillily, M. D., Reilly, L. A., & DeGrush, E. (2011). Brain ERP components predict which individuals progress to Alzheimer's disease and which do not. *Neurobiol Aging*, *32*(10), 1742-1755. https://doi.org/10.1016/j.neurobiolaging.2009.11.010

Chedid, N., Tabbal, J., Kabbara, A., Allouch, S., & Hassan, M. (2022). The development of an automated machine learning pipeline for the detection of Alzheimer's Disease. *Sci Rep*, *12*(1), 18137. https://doi.org/10.1038/s41598-022-22979-3

Choi, J., Ku, B., Doan, D. N. T., Park, J., Cha, W., Kim, J. U., & Lee, K. H. (2023). Prefrontal EEG slowing, synchronization, and ERP peak latency in association with predementia stages of Alzheimer's disease. *Front Aging Neurosci*, *15*, 1131857. https://doi.org/10.3389/fnagi.2023.1131857

Christensen, J. C., Estepp, J. R., Wilson, G. F., & Russell, C. A. (2012). The effects of day-to-day variability of physiological data on operator functional state classification. *NeuroImage*, *59*(1), 57-63. https://doi.org/10.1016/j.neuroimage.2011.07.091

Clark, C. M., Pontecorvo, M. J., Beach, T. G., Bedell, B. J., Coleman, R. E., Doraiswamy, P. M., Fleisher, A. S., Reiman, E. M., Sabbagh, M. N., Sadowsky, C. H., Schneider, J. A., Arora, A., Carpenter, A. P., Flitter, M. L., Joshi, A. D., Krautkramer, M. J., Lu, M., Mintun, M. A., & Skovronsky, D. M. (2012). Cerebral PET with florbetapir compared with neuropathology at autopsy for detection of neuritic amyloid-β plaques: a prospective cohort study. *Lancet Neurol*, *11*(8), 669-678. https://doi.org/10.1016/s1474-4422(12)70142-4

Coben, L. A., Danziger, W., & Storandt, M. (1985). A longitudinal EEG study of mild senile dementia of Alzheimer type: changes at 1 year and at 2.5 years. *Electroencephalogr Clin Neurophysiol*, *61*(2), 101-112. https://doi.org/10.1016/0013-4694(85)91048-x

Cortes, C., & Vapnik, V. (1995). Support-vector networks. *Machine Learning*, *20*(3), 273-297. https://doi.org/10.1007/BF00994018

Cummins, T. D. R., Broughton, M., & Finnigan, S. (2008). Theta oscillations are affected by amnestic mild cognitive impairment and cognitive load. *International Journal of Psychophysiology*, *70*(1), 75-81. https://doi.org/10.1016/j.ijpsycho.2008.06.002

Dauwels, J., Vialatte, F.-B., & Cichocki, A. (2011). On the Early Diagnosis of Alzheimer's Disease from EEG Signals: A Mini-Review. In R. Wang & F. Gu (Eds.), *Advances in Cognitive Neurodynamics (II)*. Springer Netherlands. https://doi.org/10.1007/978-90-481-9695-1_106

de Haan, W., Stam, C. J., Jones, B. F., Zuiderwijk, I. M., van Dijk, B. W., & Scheltens, P. (2008). Resting-state oscillatory brain dynamics in Alzheimer disease. *J Clin Neurophysiol*, *25*(4), 187-193. https://doi.org/10.1097/WNP.0b013e31817da184

Deiber, M.-P., Ibañez, V., Missonnier, P., Herrmann, F., Fazio-Costa, L., Gold, G., & Giannakopoulos, P. (2009). Abnormal-induced theta activity supports early directed-attention network deficits in progressive MCI. *Neurobiology of Aging*, *30*(9), 1444-1452. https://doi.org/10.1016/j.neurobiolaging.2007.11.021

Delorme, A., & Makeig, S. (2004). EEGLAB: an open source toolbox for analysis of single-trial EEG dynamics including independent component analysis. *J Neurosci Methods*, *134*(1), 9-21. https://doi.org/10.1016/j.jneumeth.2003.10.009

Devos, H., Burns, J. M., Liao, K., Ahmadnezhad, P., Mahnken, J. D., Brooks, W. M., & Gustafson, K. (2020). Reliability of P3 Event-Related Potential During Working Memory Across the Spectrum of Cognitive Aging. *Front Aging Neurosci*, *12*, 566391. https://doi.org/10.3389/fnagi.2020.566391

Devos, H., Gustafson, K., Liao, K., Ahmadnezhad, P., Estes, B., Martin, L. E., Mahnken, J. D., Brooks, W. M., & Burns, J. M. (2022). EEG/ERP evidence of possible hyperexcitability in older adults with elevated beta-amyloid. *Transl Neurodegener*, *11*(1), 8. https://doi.org/10.1186/s40035-022-00282-5

Devos, H., Gustafson, K. M., Liao, K., Ahmadnezhad, P., Kuhlmann, E., Estes, B. J., Martin, L. E., Mahnken, J. D., Brooks, W. M., & Burns, J. M. (2023). Effect of Cognitive Reserve on Physiological Measures of Cognitive Workload in Older Adults with Cognitive Impairments. *Journal of Alzheimer's Disease*, *92*, 141-151. https://doi.org/10.3233/JAD-220890

Di Flumeri, G., Borghini, G., Aricò, P., Sciaraffa, N., Lanzi, P., Pozzi, S., Vignali, V., Lantieri, C., Bichicchi, A., Simone, A., & Babiloni, F. (2018). EEG-Based Mental Workload Neurometric to Evaluate the Impact of Different Traffic and Road Conditions in Real Driving Settings. *Front Hum Neurosci*, *12*, 509. https://doi.org/10.3389/fnhum.2018.00509

Ding, Y., Chu, Y., Liu, M., Ling, Z., Wang, S., Li, X., & Li, Y. (2022). Fully automated discrimination of Alzheimer's disease using resting-state electroencephalography signals. *Quant Imaging Med Surg*, *12*(2), 1063-1078. https://doi.org/10.21037/qims-21-430

Faust, O., Acharya, U. R., Adeli, H., & Adeli, A. (2015). Wavelet-based EEG processing for computer-aided seizure detection and epilepsy diagnosis. *Seizure*, *26*, 56-64. https://doi.org/10.1016/j.seizure.2015.01.012

Fawcett, T. (2006). An introduction to ROC analysis. *Pattern Recognition Letters*, *27*(8), 861-874. https://doi.org/10.1016/j.patrec.2005.10.010

Fernández, A., Hornero, R., Mayo, A., Poza, J., Maestú, F., & Ortiz Alonso, T. (2006). Quantitative magnetoencephalography of spontaneous brain activity in Alzheimer disease: an exhaustive frequency analysis. *Alzheimer Dis Assoc Disord*, *20*(3), 153-159. https://doi.org/10.1097/00002093-200607000-00006

Fiscon, G., Weitschek, E., Cialini, A., Felici, G., Bertolazzi, P., De Salvo, S., Bramanti, A., Bramanti, P., & De Cola, M. C. (2018). Combining EEG signal processing with supervised methods for Alzheimer's patients classification. *BMC Medical Informatics and Decision Making*, *18*(1), 35. https://doi.org/10.1186/s12911-018-0613-y

Fraga, F. J., Mamani, G. Q., Johns, E., Tavares, G., Falk, T. H., & Phillips, N. A. (2018). Early diagnosis of mild cognitive impairment and Alzheimer's with event-related potentials and

event-related desynchronization in N-back working memory tasks. *Comput Methods Programs Biomed*, *164*, 1-13. https://doi.org/10.1016/j.cmpb.2018.06.011

Frantzidis, C. A., Vivas, A. B., Tsolaki, A., Klados, M. A., Tsolaki, M., & Bamidis, P. D. (2014). Functional disorganization of small-world brain networks in mild Alzheimer's Disease and amnestic Mild Cognitive Impairment: an EEG study using Relative Wavelet Entropy (RWE). *Front Aging Neurosci*, *6*, 224. https://doi.org/10.3389/fnagi.2014.00224

Ghorbanian, P., Devilbiss, D. M., Verma, A., Bernstein, A., Hess, T., Simon, A. J., & Ashrafiuon, H. (2013). Identification of resting and active state EEG features of Alzheimer's disease using discrete wavelet transform. *Ann Biomed Eng*, *41*(6), 1243-1257. https://doi.org/10.1007/s10439-013-0795-5

Gómez, C., Stam, C. J., Hornero, R., Fernández, A., & Maestú, F. (2009). Disturbed beta band functional connectivity in patients with mild cognitive impairment: an MEG study. *IEEE Trans Biomed Eng*, *56*(6), 1683-1690. https://doi.org/10.1109/tbme.2009.2018454

Gouw, A. A., Alsema, A. M., Tijms, B. M., Borta, A., Scheltens, P., Stam, C. J., & van der Flier, W. M. (2017). EEG spectral analysis as a putative early prognostic biomarker in nondemented, amyloid positive subjects. *Neurobiol Aging*, *57*, 133-142. https://doi.org/10.1016/j.neurobiolaging.2017.05.017

Grootswagers, T., Wardle, S. G., & Carlson, T. A. (2017). Decoding Dynamic Brain Patterns from Evoked Responses: A Tutorial on Multivariate Pattern Analysis Applied to Time Series Neuroimaging Data. *J Cogn Neurosci*, *29*(4), 677-697. https://doi.org/10.1162/jocn_a_01068

Harmony, T. (2013). The functional significance of delta oscillations in cognitive processing. *Front Integr Neurosci*, *7*, 83. https://doi.org/10.3389/fnint.2013.00083

Harmony, T., Fernández, T., Silva, J., Bernal, J., Díaz-Comas, L., Reyes, A., Marosi, E., Rodríguez, M., & Rodríguez, M. (1996). EEG delta activity: an indicator of attention to internal processing during performance of mental tasks. *International Journal of Psychophysiology*, *24*(1), 161-171. https://doi.org/10.1016/S0167-8760(96)00053-0

Harn, N. R., Hunt, S. L., Hill, J., Vidoni, E., Perry, M., & Burns, J. M. (2017). Augmenting Amyloid PET Interpretations With Quantitative Information Improves Consistency of Early Amyloid Detection. *Clin Nucl Med*, *42*(8), 577-581. https://doi.org/10.1097/rlu.0000000000001693

Horvath, A., Szucs, A., Csukly, G., Sakovics, A., Stefanics, G., & Kamondi, A. (2018). EEG and ERP biomarkers of Alzheimer's disease: a critical review. *Front Biosci (Landmark Ed)*, *23*(2), 183-220. https://doi.org/10.2741/4587

Imaruoka, T., Saiki, J., & Miyauchi, S. (2005). Maintaining coherence of dynamic objects requires coordination of neural systems extended from anterior frontal to posterior parietal brain cortices. *NeuroImage*, *26*(1), 277-284. https://doi.org/10.1016/j.neuroimage.2005.01.045

Ishii, R., Canuet, L., Aoki, Y., Hata, M., Iwase, M., Ikeda, S., Nishida, K., & Ikeda, M. (2017). Healthy and Pathological Brain Aging: From the Perspective of Oscillations, Functional Connectivity, and Signal Complexity. *Neuropsychobiology*, *75*(4), 151-161. https://doi.org/10.1159/000486870

Jack, C. R., Jr., Knopman, D. S., Jagust, W. J., Petersen, R. C., Weiner, M. W., Aisen, P. S., Shaw, L. M., Vemuri, P., Wiste, H. J., Weigand, S. D., Lesnick, T. G., Pankratz, V. S., Donohue, M. C., & Trojanowski, J. Q. (2013). Tracking pathophysiological processes in Alzheimer's disease: an updated hypothetical model of dynamic biomarkers. *Lancet Neurol*, *12*(2), 207-216. https://doi.org/10.1016/s1474-4422(12)70291-0

Jack, C. R., Jr., Knopman, D. S., Jagust, W. J., Shaw, L. M., Aisen, P. S., Weiner, M. W., Petersen, R. C., & Trojanowski, J. Q. (2010). Hypothetical model of dynamic biomarkers of the Alzheimer's pathological cascade. *Lancet Neurol*, *9*(1), 119-128. https://doi.org/10.1016/s1474-4422(09)70299-6

James, G. W., Daniela; Hastie, Trevor; Tibshirani, Robert. (2021). *An Introduction to Statistical Learning: with Applications in R* (2nd ed.). Springer.

Jiang, Z. Y. (2005). Study on EEG power and coherence in patients with mild cognitive impairment during working memory task. *J Zhejiang Univ Sci B*, *6*(12), 1213-1219. https://doi.org/10.1631/jzus.2005.B1213

Joshi, A. D., Pontecorvo, M. J., Clark, C. M., Carpenter, A. P., Jennings, D. L., Sadowsky, C. H., Adler, L. P., Kovnat, K. D., Seibyl, J. P., Arora, A., Saha, K., Burns, J. D., Lowrey, M. J., Mintun, M. A., & Skovronsky, D. M. (2012). Performance characteristics of amyloid PET with florbetapir F 18 in patients with alzheimer's disease and cognitively normal subjects. *J Nucl Med*, *53*(3), 378-384. https://doi.org/10.2967/jnumed.111.090340

Karrasch, M., Laine, M., Rinne, J. O., Rapinoja, P., Sinervä, E., & Krause, C. M. (2006). Brain oscillatory responses to an auditory-verbal working memory task in mild cognitive impairment and Alzheimer's disease. *Int J Psychophysiol*, *59*(2), 168-178. https://doi.org/10.1016/j.ijpsycho.2005.04.006

Khatri, U., & Kwon, G. R. (2022). Alzheimer's Disease Diagnosis and Biomarker Analysis Using Resting-State Functional MRI Functional Brain Network With Multi-Measures Features and Hippocampal Subfield and Amygdala Volume of Structural MRI. *Front Aging Neurosci*, *14*, 818871. https://doi.org/10.3389/fnagi.2022.818871

Khatun, S., Morshed, B. I., & Bidelman, G. M. (2019). A Single-Channel EEG-Based Approach to Detect Mild Cognitive Impairment via Speech-Evoked Brain Responses. *IEEE Trans Neural Syst Rehabil Eng*, *27*(5), 1063-1070. https://doi.org/10.1109/tnsre.2019.2911970

King, J. R., & Dehaene, S. (2014). Characterizing the dynamics of mental representations: the temporal generalization method. *Trends Cogn Sci*, *18*(4), 203-210. https://doi.org/10.1016/j.tics.2014.01.002

Kondo, H., Morishita, M., Osaka, N., Osaka, M., Fukuyama, H., & Shibasaki, H. (2004). Functional roles of the cingulo-frontal network in performance on working memory. *NeuroImage*, *21*(1), 2-14. https://doi.org/10.1016/j.neuroimage.2003.09.046

Kurt, P., Emek-Savaş, D. D., Batum, K., Turp, B., Güntekin, B., Karşıdağ, S., & Yener, G. G. (2014). Patients with Mild Cognitive Impairment Display Reduced Auditory Event-Related Delta Oscillatory Responses. *Behavioural Neurology*, *2014*, 268967. https://doi.org/10.1155/2014/268967

Lai, C. L., Lin, R. T., Liou, L. M., & Liu, C. K. (2010). The role of event-related potentials in cognitive decline in Alzheimer's disease. *Clin Neurophysiol*, *121*(2), 194-199. https://doi.org/10.1016/j.clinph.2009.11.001

Li, X., Liu, Y., Kang, J., Sun, Y., Xu, Y., Yuan, Y., Han, Y., & Xie, P. (2022). Identifying Amnestic Mild Cognitive Impairment With Convolutional Neural Network Adapted to the Spectral Entropy Heat Map of the Electroencephalogram. *Front Hum Neurosci*, *16*, 924222. https://doi.org/10.3389/fnhum.2022.924222

Liu, J., Li, M., Lan, W., Wu, F. X., Pan, Y., & Wang, J. (2018). Classification of Alzheimer's Disease Using Whole Brain Hierarchical Network. *IEEE/ACM Trans Comput Biol Bioinform*, *15*(2), 624-632. https://doi.org/10.1109/tcbb.2016.2635144

Maestú, F., Cuesta, P., Hasan, O., Fernandéz, A., Funke, M., & Schulz, P. E. (2019). The Importance of the Validation of M/EEG With Current Biomarkers in Alzheimer's Disease. *Front Hum Neurosci*, *13*, 17. https://doi.org/10.3389/fnhum.2019.00017

Mazaheri, A., Segaert, K., Olichney, J., Yang, J. C., Niu, Y. Q., Shapiro, K., & Bowman, H. (2018). EEG oscillations during word processing predict MCI conversion to Alzheimer's disease. *Neuroimage Clin*, *17*, 188-197. https://doi.org/10.1016/j.nicl.2017.10.009

Meghdadi, A. H., Stevanović Karić, M., McConnell, M., Rupp, G., Richard, C., Hamilton, J., Salat, D., & Berka, C. (2021). Resting state EEG biomarkers of cognitive decline associated with Alzheimer's disease and mild cognitive impairment. *PLoS One*, *16*(2), e0244180. https://doi.org/10.1371/journal.pone.0244180

Menagadevi, M., Mangai, S., Madian, N., & Thiyagarajan, D. (2023). Automated prediction system for Alzheimer detection based on deep residual autoencoder and support vector machine. *Optik*, *272*, 170212. https://doi.org/10.1016/j.ijleo.2022.170212

Michels, L., Bucher, K., Lüchinger, R., Klaver, P., Martin, E., Jeanmonod, D., & Brandeis, D. (2010). Simultaneous EEG-fMRI during a Working Memory Task: Modulations in Low and High Frequency Bands. *PLoS One*, *5*(4), e10298. https://doi.org/10.1371/journal.pone.0010298

Miller, E. K., Lundqvist, M., & Bastos, A. M. (2018). Working Memory 2.0. *Neuron*, *100*(2), 463-475. https://doi.org/10.1016/j.neuron.2018.09.023

Mirzaei, G., & Adeli, H. (2022). Machine learning techniques for diagnosis of alzheimer disease, mild cognitive disorder, and other types of dementia. *Biomedical Signal Processing and Control*, *72*, 103293. https://doi.org/10.1016/j.bspc.2021.103293

Missonnier, P., Deiber, M. P., Gold, G., Herrmann, F. R., Millet, P., Michon, A., Fazio-Costa, L., Ibañez, V., & Giannakopoulos, P. (2007). Working memory load-related electroencephalographic parameters can differentiate progressive from stable mild cognitive impairment. *Neuroscience*, *150*(2), 346-356. https://doi.org/10.1016/j.neuroscience.2007.09.009

Missonnier, P., Gold, G., Herrmann, F. R., Fazio-Costa, L., Michel, J. P., Deiber, M. P., Michon, A., & Giannakopoulos, P. (2006). Decreased theta event-related synchronization during working memory activation is associated with progressive mild cognitive impairment. *Dement Geriatr Cogn Disord*, *22*(3), 250-259. https://doi.org/10.1159/000094974

Moretti, D. V. (2016). Electroencephalography-driven approach to prodromal Alzheimer's disease diagnosis: from biomarker integration to network-level comprehension. *Clin Interv Aging*, *11*, 897-912. https://doi.org/10.2147/cia.S103313

Moretti, D. V., Babiloni, C., Binetti, G., Cassetta, E., Dal Forno, G., Ferreric, F., Ferri, R., Lanuzza, B., Miniussi, C., Nobili, F., Rodriguez, G., Salinari, S., & Rossini, P. M. (2004). Individual analysis of EEG frequency and band power in mild Alzheimer's disease. *Clinical Neurophysiology*, *115*(2), 299-308. https://doi.org/10.1016/S1388-2457(03)00345-6

Moscoso, A., Silva-Rodríguez, J., Aldrey, J. M., Cortés, J., Fernández-Ferreiro, A., Gómez-Lado, N., Ruibal, Á., & Aguiar, P. (2019). Prediction of Alzheimer's disease dementia with MRI beyond the short-term: Implications for the design of predictive models. *NeuroImage: Clinical*, *23*, 101837. https://doi.org/10.1016/j.nicl.2019.101837

Murugappan, M., Ramachandran, N., & Sazali, Y. (2010). Classification of human emotion from EEG using discrete wavelet transform. *Journal of Biomedical Science and Engineering*, *3*(4), 390-396, Article 1607. https://doi.org/10.4236/jbise.2010.34054

Nakamura, A., Cuesta, P., Fernández, A., Arahata, Y., Iwata, K., Kuratsubo, I., Bundo, M., Hattori, H., Sakurai, T., Fukuda, K., Washimi, Y., Endo, H., Takeda, A., Diers, K., Bajo, R., Maestú, F., Ito, K., & Kato, T. (2018). Electromagnetic signatures of the preclinical and prodromal stages of Alzheimer's disease. *Brain*, *141*(5), 1470-1485. https://doi.org/10.1093/brain/awy044

Nasreddine, Z. S., Phillips, N. A., Bédirian, V., Charbonneau, S., Whitehead, V., Collin, I., Cummings, J. L., & Chertkow, H. (2005). The Montreal Cognitive Assessment, MoCA: a brief screening tool for mild cognitive impairment. *J Am Geriatr Soc*, *53*(4), 695-699. https://doi.org/10.1111/j.1532-5415.2005.53221.x

Ouchani, M., Gharibzadeh, S., Jamshidi, M., & Amini, M. (2021). A Review of Methods of Diagnosis and Complexity Analysis of Alzheimer's Disease Using EEG Signals. *Biomed Res Int*, *2021*, 5425569. https://doi.org/10.1155/2021/5425569

Owen, A. M., McMillan, K. M., Laird, A. R., & Bullmore, E. (2005). N-back working memory paradigm: a meta-analysis of normative functional neuroimaging studies. *Hum Brain Mapp*, *25*(1), 46-59. https://doi.org/10.1002/hbm.20131

Patterson, C. (2018). *World Alzheimer Report 2018. The state of the art of dementia research: New frontiers*. Alzheimer's Disease International.

Pellegrini, E., Ballerini, L., Hernandez, M., Chappell, F. M., González-Castro, V., Anblagan, D., Danso, S., Muñoz-Maniega, S., Job, D., Pernet, C., Mair, G., MacGillivray, T. J., Trucco, E., & Wardlaw, J. M. (2018). Machine learning of neuroimaging for assisted diagnosis of cognitive impairment and dementia: A systematic review. *Alzheimers Dement (Amst)*, *10*, 519-535. https://doi.org/10.1016/j.dadm.2018.07.004

Perez-Valero, E., Lopez-Gordo, M. A., Morillas, C., Pelayo, F., & Vaquero-Blasco, M. A. (2021). A Review of Automated Techniques for Assisting the Early Detection of Alzheimer's Disease with a Focus on EEG. *J Alzheimers Dis*, *80*(4), 1363-1376. https://doi.org/10.3233/jad-201455

Pesonen, M., Hämäläinen, H., & Krause, C. M. (2007). Brain oscillatory 4-30 Hz responses during a visual n-back memory task with varying memory load. *Brain Res*, *1138*, 171-177. https://doi.org/10.1016/j.brainres.2006.12.076

Petrosian, A. A., Prokhorov, D. V., Lajara-Nanson, W., & Schiffer, R. B. (2001). Recurrent neural network-based approach for early recognition of Alzheimer's disease in EEG. *Clin Neurophysiol*, *112*(8), 1378-1387. https://doi.org/10.1016/s1388-2457(01)00579-x

Polikar, R., Topalis, A., Green, D., Kounios, J., & Clark, C. M. (2007). Comparative multiresolution wavelet analysis of ERP spectral bands using an ensemble of classifiers approach for early diagnosis of Alzheimer's disease. *Comput Biol Med*, *37*(4), 542-558. https://doi.org/10.1016/j.compbiomed.2006.08.012

Poza, J., Gómez, C., García, M., Corralejo, R., Fernández, A., & Hornero, R. (2014). Analysis of neural dynamics in mild cognitive impairment and Alzheimer's disease using wavelet turbulence. *J Neural Eng*, *11*(2), 026010. https://doi.org/10.1088/1741-2560/11/2/026010

Rathore, S., Habes, M., Iftikhar, M. A., Shacklett, A., & Davatzikos, C. (2017). A review on neuroimaging-based classification studies and associated feature extraction methods for Alzheimer's disease and its prodromal stages. *NeuroImage*, *155*, 530-548. https://doi.org/10.1016/j.neuroimage.2017.03.057

Rossini, P. M., Rossi, S., Babiloni, C., & Polich, J. (2007). Clinical neurophysiology of aging brain: from normal aging to neurodegeneration. *Prog Neurobiol*, *83*(6), 375-400. https://doi.org/10.1016/j.pneurobio.2007.07.010

Rosso, O. A., Martin, M. T., Figliola, A., Keller, K., & Plastino, A. (2006). EEG analysis using wavelet-based information tools. *J Neurosci Methods*, *153*(2), 163-182. https://doi.org/10.1016/j.jneumeth.2005.10.009

Sajda, P. (2006). Machine learning for detection and diagnosis of disease. *Annu Rev Biomed Eng*, *8*, 537-565. https://doi.org/10.1146/annurev.bioeng.8.061505.095802

Schmidt, R., Herrojo Ruiz, M., Kilavik, B. E., Lundqvist, M., Starr, P. A., & Aron, A. R. (2019). Beta Oscillations in Working Memory, Executive Control of Movement and Thought, and Sensorimotor Function. *J Neurosci*, *39*(42), 8231-8238. https://doi.org/10.1523/jneurosci.1163-19.2019

Sibilano, E., Brunetti, A., Buongiorno, D., Lassi, M., Grippo, A., Bessi, V., Micera, S., Mazzoni, A., & Bevilacqua, V. (2023). An attention-based deep learning approach for the classification of subjective cognitive decline and mild cognitive impairment using resting-state EEG. *J Neural Eng*, *20*(1). https://doi.org/10.1088/1741-2552/acb96e

Smailovic, U., & Jelic, V. (2019). Neurophysiological Markers of Alzheimer's Disease: Quantitative EEG Approach. *Neurol Ther*, *8*(Suppl 2), 37-55. https://doi.org/10.1007/s40120-019-00169-0

Spitzer, B., & Haegens, S. (2017). Beyond the Status Quo: A Role for Beta Oscillations in Endogenous Content (Re)Activation. *eNeuro*, *4*(4). https://doi.org/10.1523/eneuro.0170-17.2017

Stam, C. J., Montez, T., Jones, B. F., Rombouts, S. A., van der Made, Y., Pijnenburg, Y. A., & Scheltens, P. (2005). Disturbed fluctuations of resting state EEG synchronization in Alzheimer's disease. *Clin Neurophysiol*, *116*(3), 708-715. https://doi.org/10.1016/j.clinph.2004.09.022

Stomrud, E., Hansson, O., Minthon, L., Blennow, K., Rosén, I., & Londos, E. (2010). Slowing of EEG correlates with CSF biomarkers and reduced cognitive speed in elderly with normal cognition over 4 years. *Neurobiol Aging*, *31*(2), 215-223. https://doi.org/10.1016/j.neurobiolaging.2008.03.025

Strang, G., & Nguyen, T. (1996). *Wavelets and Filter Banks* (2nd ed.). Wellesley-Cambridge Press.

Subasi, A. (2007). EEG signal classification using wavelet feature extraction and a mixture of expert model. *Expert Systems with Applications*, *32*(4), 1084-1093. https://doi.org/10.1016/j.eswa.2006.02.005

Tanveer, M., Richhariya, B., Khan, R. U., Rashid, A. H., Khanna, P., Prasad, M., & Lin, C. T. (2020). Machine Learning Techniques for the Diagnosis of Alzheimer's Disease: A Review. *ACM Trans. Multimedia Comput. Commun. Appl.*, *16*(1s), 1-35. https://doi.org/10.1145/3344998

Targa Dias Anastacio, H., Matosin, N., & Ooi, L. (2022). Neuronal hyperexcitability in Alzheimer's disease: what are the drivers behind this aberrant phenotype? *Transl Psychiatry*, *12*(1), 257. https://doi.org/10.1038/s41398-022-02024-7

Trambaiolli, L. R., Lorena, A. C., Fraga, F. J., Kanda, P. A., Anghinah, R., & Nitrini, R. (2011). Improving Alzheimer's disease diagnosis with machine learning techniques. *Clin EEG Neurosci*, *42*(3), 160-165. https://doi.org/10.1177/155005941104200304

Treder, M. S. (2020). MVPA-Light: A Classification and Regression Toolbox for Multi-Dimensional Data. *Front Neurosci*, *14*, 289. https://doi.org/10.3389/fnins.2020.00289

Trinh, T. T., Tsai, C. F., Hsiao, Y. T., Lee, C. Y., Wu, C. T., & Liu, Y. H. (2021). Identifying Individuals With Mild Cognitive Impairment Using Working Memory-Induced Intra-Subject Variability of Resting-State EEGs. *Front Comput Neurosci*, *15*, 700467. https://doi.org/10.3389/fncom.2021.700467

van der Hiele, K., Vein, A. A., Kramer, C. G., Reijntjes, R. H., van Buchem, M. A., Westendorp, R. G., Bollen, E. L., van Dijk, J. G., & Middelkoop, H. A. (2007). Memory activation enhances EEG abnormality in mild cognitive impairment. *Neurobiol Aging*, *28*(1), 85-90. https://doi.org/10.1016/j.neurobiolaging.2005.11.006

Vidoni, E. D., Morris, J. K., Watts, A., Perry, M., Clutton, J., Van Sciver, A., Kamat, A. S., Mahnken, J., Hunt, S. L., Townley, R., Honea, R., Shaw, A. R., Johnson, D. K., Vacek, J., & Burns, J. M. (2021). Effect of aerobic exercise on amyloid accumulation in preclinical Alzheimer's: A 1-year randomized controlled trial. *PLoS One*, *16*(1), e0244893. https://doi.org/10.1371/journal.pone.0244893

Wan, B., Ming, D., Fu, X., Yang, C., Qi, H., & Chen, B. (2006). Study on a quantitative electroencephalography power spectrum typical of Chinese Han Alzheimer's disease patients by using wavelet transforms. *J Neural Eng*, *3*(1), 71-77. https://doi.org/10.1088/1741-2560/3/1/008

Wang, S., Gwizdka, J., & Chaovalitwongse, W. A. (2016). Using Wireless EEG Signals to Assess Memory Workload in the n-Back Task. *IEEE Transactions on Human-Machine Systems*, *46*(3), 424-435. https://doi.org/10.1109/THMS.2015.2476818

Yener, G. G., & Başar, E. (2013). Biomarkers in Alzheimer's disease with a special emphasis on event-related oscillatory responses. *Suppl Clin Neurophysiol*, *62*, 237-273. https://doi.org/10.1016/b978-0-7020-5307-8.00020-x

Yener, G. G., Kurt, P., Emek-Savaş, D. D., Güntekin, B., & Başar, E. (2013). Reduced Visual Event-Related Delta Oscillatory Responses in Amnestic Mild Cognitive Impairment. *Journal of Alzheimer's Disease*, *37*, 759-767. https://doi.org/10.3233/JAD-130569

You, Z., Zeng, R., Lan, X., Ren, H., You, Z., Shi, X., Zhao, S., Guo, Y., Jiang, X., & Hu, X. (2020). Alzheimer's Disease Classification With a Cascade Neural Network. *Front Public Health*, *8*, 584387. https://doi.org/10.3389/fpubh.2020.584387

Zarjam, P., Epps, J., & Lovell, N. H. (2015). Beyond Subjective Self-Rating: EEG Signal Classification of Cognitive Workload. *IEEE Transactions on Autonomous Mental Development*, *7*(4), 301-310. https://doi.org/10.1109/TAMD.2015.2441960